Available online at www.sciencedirect.com

ScienceDirect

journal homepage: www.elsevier.com/locate/he

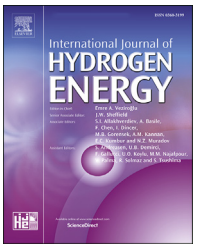

Flexible production of green hydrogen and ammonia from variable solar and wind energy: Case study of Chile and Argentina

Julien Armijo [a,*], *Cédric Philibert* [b]

[a] *Centro de Investigación en Recursos Naturales y Sustentabilidad, Universidad Bernardo O'Higgins, Santiago, Chile*
[b] *International Energy Agency, OECD, Paris, France*

HIGHLIGHTS

- World-class solar and wind in Chile and Argentina allow for competitive green H_2 and NH_3 production.
- Combining wind and solar can reduce costs especially for NH_3 production.
- Renewable power variability is a major cost driver for NH_3 synthesis.
- Flexibiliy in NH_3 synthesis is key to manage the variability.

ARTICLE INFO

Article history:
Received 20 May 2019
Received in revised form
11 October 2019
Accepted 6 November 2019
Available online xxx

Keywords:
Energy transition
Renewable energy
Hydrogen
Ammonia
Flexibility

ABSTRACT

We report a techno-economic modelling for the flexible production of hydrogen and ammonia from water and optimally combined solar and wind energy. We use hourly data in four locations with world-class solar in the Atacama desert and wind in Patagonia steppes. We find that hybridization of wind and solar can reduce hydrogen production costs by a few percents, when the effect of increasing the load factor on the electrolyser overweighs the electricity cost increase. For ammonia production, the gains by hybridization can be substantially larger, because it reduces the power variability, which is costly, due to the need for intermediate storage of hydrogen between the flexible electrolyser and the less flexible ammonia synthesis unit. Our modelling reveals the crucial role in the synthesis of flexibility, which cuts the cost of variability, especially for the more variable wind power. Our estimated near-term production costs for green hydrogen, around 2 USD/kg, and green ammonia, below 500 USD/t, are encouragingly close to competitiveness against fossil-fuel alternatives.

Introduction

Since recent studies have shown that climate change is becoming an "existential threat" to humanity, with possible warming above 2 °C in the next three decades and beyond 4 °C–6 °C within the next several decades [1], it has become clear that aggressive reductions of greenhouse gas emissions to near zero level must be implemented as soon as possible to avoid global warming turning from dangerous to catastrophic [2–4].

* *Corresponding author.*
E-mail addresses: julienarmijo@gmail.com (J. Armijo), blogcedricphilibert@gmail.com (C. Philibert).
https://doi.org/10.1016/j.ijhydene.2019.11.028

Please cite this article as: Armijo J, Philibert C, Flexible production of green hydrogen and ammonia from variable solar and wind energy: Case study of Chile and Argentina, International Journal of Hydrogen Energy, https://doi.org/10.1016/j.ijhydene.2019.11.028

To address this challenge, renewable electricity and biomass are not sufficient. Green hydrogen production via water electrolysis is the paradigm of industrial conversion of renewable electricity into chemical energy, storable and transportable. As such, water electrolysis and the conversion of green electricity into heavier green molecules and fuels beyond hydrogen, is attracting rapidly increasing attention, because of the promise of unleashing the potential of low-emission renewable energies (RE) way beyond electricity, and pave the way for realistic planning of a global economy with net zero emissions [5–9].

However, a key remaining question concerns the temporal variability of wind and solar, the main resources expected to play the largest role in the increase of RE in the global energy system (see, e.g. Ref. [10]). How does their variability affect the production costs of H_2, NH_3 or carbon-based synthetic fuels? Some studies, like [11] for methane, or [12] for methanol, have found that if the steps after the electrolysis are not flexible, the required intermediate buffer storage of H_2 could be a prominent cost driver. Yet, most previous studies modelling green hydrogen or green fuels production, have avoided to treat the variability issue, assuming either dispatchable RE power from the grid (e.g. Ref. [13], for ammonia), perfectly flexible synthesis (e.g. Ref. [14], for ammonia), or underground buffer storage of hydrogen, which is so cheap that it almost erases the cost of variability (e.g. Ref. [15], for Fischer-Tropsch fuels). For ammonia, flexible production was modelled in Ref. [16] wind power from grid with 80% down flexibility, and in Ref. [17] from an islanded wind farm and flexibility varied from 0% to 80%. A complete understanding of the role of flexibility is thus still in progress, especially when considering also the open question of the possible interest to combine wind and solar power, as suggested, e.g., in Ref. [15] to reduce the variability of the hybrid power mix, and thus reduce the production costs of green synthetic fuels.

In this paper, we present a techno-economic model that plainly addresses these questions, using four example locations in Chile and Argentina, two countries having world-class variable renewable energy (VRE) resources, and thus tremendous potentials for becoming leading RE producers, and exporters of RE stored in H-rich chemicals [8,18]. Chile has the world's strongest solar resource and good wind in the north, and excellent wind in the far south. Argentina has among the world's best onshore wind potentials in its vast desert Patagonian steppes, and very good solar in the North.

For each location, our modelling estimates the short-term costs of mass production of H_2 and NH_3 based on full meteorological yearly data with hourly resolution, determining the optimal relative sizes of the solar, wind and NH_3-synthesis units, for a fixed electrolyser size. We focus on NH_3 because, apart from H_2 itself (and the more complex hydrazine), it is the only potential H-based fuel that does not contain carbon. It is easier to liquefy, store and transport than H_2, and has a greater energy density. Furthermore, it is a large global market already, internationally traded with pipelines and oceangoing tankers [19,20]. However, the production of 1 tNH_3 from natural gas (resp. coal) currently entails emission of 2.3 tCO_2 (resp. 3.9 tCO_2), while the production of 1 tH_2 from gas (resp.coal) emits 10 tCO_2 (resp. 19 tCO_2) [6].

Our goal is essentially to treat the situation of abundant and cheap renewable resources, in locations far from consumption centers [5] where grids are generally weak, therefore, our modelling is based on dedicated wind and solar resources, so that we face the questions of variability completely. Our modelling allows to understand the benefits of hybridization of wind and solar power, which is much stronger when the less flexible process of ammonia synthesis follows the production of hydrogen. We also analyse the interplay between the variability of the RE sources, the flexibility of the ammonia plant, and the optimal sizing of the wind, solar, and ammonia synthesis units.

The potential for renewables in Chile and Argentina

Chile

In Chile, the potential for renewable electricity production via solar PV, CSP, wind, and hydro, has been estimated in a comprehensive overview study [21], carried by the Ministry of Energy and GIZ. The study covered the country from Arica to Chiloé, that is, from the northern end of the country, to the southern end of the National Electric System (SEN). Southern Patagonian parts of Chile have two islanded electric systems.

Fig. 1 shows the capacity factors estimated in Ref. [21] for solar PV with 1-axis tracking (left), and wind (right), in the northern part of the country. In both cases, the map on the right side takes into account land restrictions (national parks, vicinity <1 km to towns, excessive elevation >2000 m, etc.). The results shown are based on meteorological Weather Research and Forecast (WRF) simulations, and technical performance of solar panels and wind turbines are computed with realistic models that include temperature dependence of solar panel efficiency, air density dependence of wind turbine efficiency, etc. In Ref. [21], the simulation results were compared in detail to field meteorological and plant production data in several representative cases, giving good reliability to the model.

In Fig. 1, estimated solar potentials reach capacity factors *CF* up to 40%, taking into account an assumption of 15% of annual technical losses. In Ref. [21], the solar potential in the North of Chile, was estimated to 1260 GW for PV and 550 GW for CSP, i.e., a total above 1800 GW available in North of Chile, considering only capacity factors $CF > 30\%$, and with a conservative land use assumption of 20 MW/km^2 (projects often reach 50 MW/km^2).

In Ref. [21], wind potentials were estimated from the model, to which a correcting factor of $0.75 = 0.85 \times 0.88$ was applied to take into account technical losses (assumed at 15%) and where the factor 0.88 accounts for the noted overestimation of the modelled wind speeds, with regards to measurements (using a station in the Taltal area). Following this procedure, the map in Fig. 1 shows potential capacity factors above 40% in several areas of the North, especially near Taltal, where wind average speeds of about 10 m/s at 80 m height were recorded in 2010 ([21] p. 21), and in several valleys such as the Calama valley. Note, however, that the specific

Please cite this article as: Armijo J, Philibert C, Flexible production of green hydrogen and ammonia from variable solar and wind energy: Case study of Chile and Argentina, International Journal of Hydrogen Energy, https://doi.org/10.1016/j.ijhydene.2019.11.028

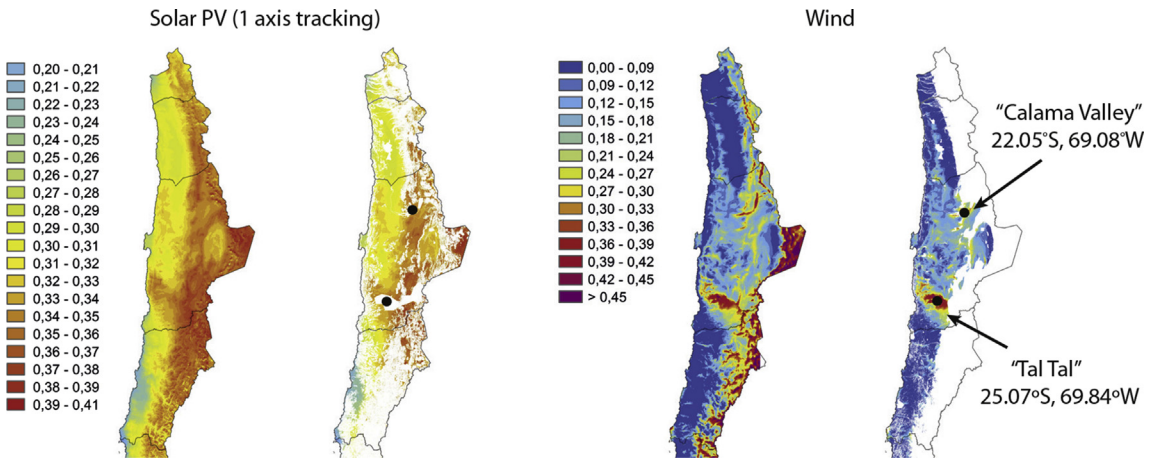

Fig. 1 – Potential capacity factors for solar and wind energy in the North of Chile. Maps on the right side show the resource combined with land restrictions. Source: [GIZ 2014].

power (i.e. power over swept area) of wind turbines considered was not specified in this work.

The available wind potential in the 5 northernmost regions shown in Fig. 1, considering only capacity factors >30%, and a typical land use of 10 MW/km^2, was estimated to about 14.5 GW, including 11.5 GW in the interior of Taltal. Very windy places on the Altiplano plateau near the border with Argentina were discarded due to excessive elevation and remoteness. Wind potentials with *CF*>40% are also available in several locations in the central North and central South, in particular, about 23 GW were identified in the southern regions of Bio-Bio, Araucanía, Los Rios, and Los Lagos (including Chiloé island), essentially along the Pacific coast or the coastal mountain ranges (see Fig. 17 in Ref. [21]) However the best wind resource with excellent potentials and capacity factors *CF*>60%, are located in the Patagonian far South (Magallanes region).

From Fig. 1 it is clear that the North of Chile offers highly interesting possibilities for solar, wind, or combinations of them. In this study, we pick two locations (see Fig. 1 and Table 1) with excellent solar resource and also very good wind ("Taltal"), or good wind ("Calama"). It also is very convenient that the Ministry of Energy disclosed two online explorer tools [22,23] that allow to simulate the production of solar and wind farms and download hourly data, with various technological assumptions. Note that the wind explorer covers the whole country, including the far southern Patagonian regions and parts of Argentina.

Argentina

For Argentina, the work [24] provided overviews of the solar and wind potentials, reproduced in Fig. 2. Schematically, most of the southern half of the country has enormous wind power with average wind speeds above 10 m/s in extensive areas, and potential capacity factors often exceeding 60%, even for class 1 turbines. The north-western part of the country, next to the Andes mountains, is arid and boasts high solar irradiation above 5.5 kWh/m^2 day, very close to the levels reached in Chile. The potentials for wind and solar in Argentina can also be visualized in Refs. [25,26].

To explore the possibility to use both the extreme wind and good solar potentials, we select a "Patagonia Argentina" location marked as red spot on Fig. 2, in the western Chubut province, and the red spot in the Chilean Magallanes region denotes the "Patagonia Chile" study case (see Table 1).

Energy situation and strategies for renewables and hydrogen

Current energy situations in Chile and Argentina

In Argentina, the primary energy matrix is strongly dominated by a 90% share of fossil fuels, including 52% of gas in 2016 [27]. In Chile, fossils are also well dominant, providing 70% of the primary energy in 2016, but biomass provided 18.5% in Chile, versus 4% in Argentina, and hydro provided 5% in 2016 in Chile, and 3.5% in Argentina. Geothermal and non-conventional renewables are rising rapidly [28], although in 2016 they provided only 1.1% of the primary energy in Chile and 0.06% in Argentina.

As reported in Ref. [29], the electrical installed capacity in Chile is 23.3 GW, with already 2.3 GW of solar, 1.5 GW of wind, 6.8 GW of hydro, 500 MW of biomass. The total annual production is about 80 TWh. Due to rapid development of variable renewable energies (VRE) in recent years (and transmission issues), electricity prices have fallen strongly in some nodes in the northern parts of the former Central Interconnected System (SIC). For example, as reported in Ref. [30], in December 2017 the Diego de Almagro spot price averaged approximately 7 USD/MWh between 11am and 6pm.

In Argentina, the installed electric capacity was 34 GW in 2017, and the total generation about 150 TWh [28]. In Argentina, renewables have just started to boom in 2018. The Argentinian wind market was in 2018 the fastest growing globally, with an installed capacity growing 181%, from 228 MW to 640 MW during 2018 [31]. 2018 also saw the first

Please cite this article as: Armijo J, Philibert C, Flexible production of green hydrogen and ammonia from variable solar and wind energy: Case study of Chile and Argentina, International Journal of Hydrogen Energy, https://doi.org/10.1016/j.ijhydene.2019.11.028

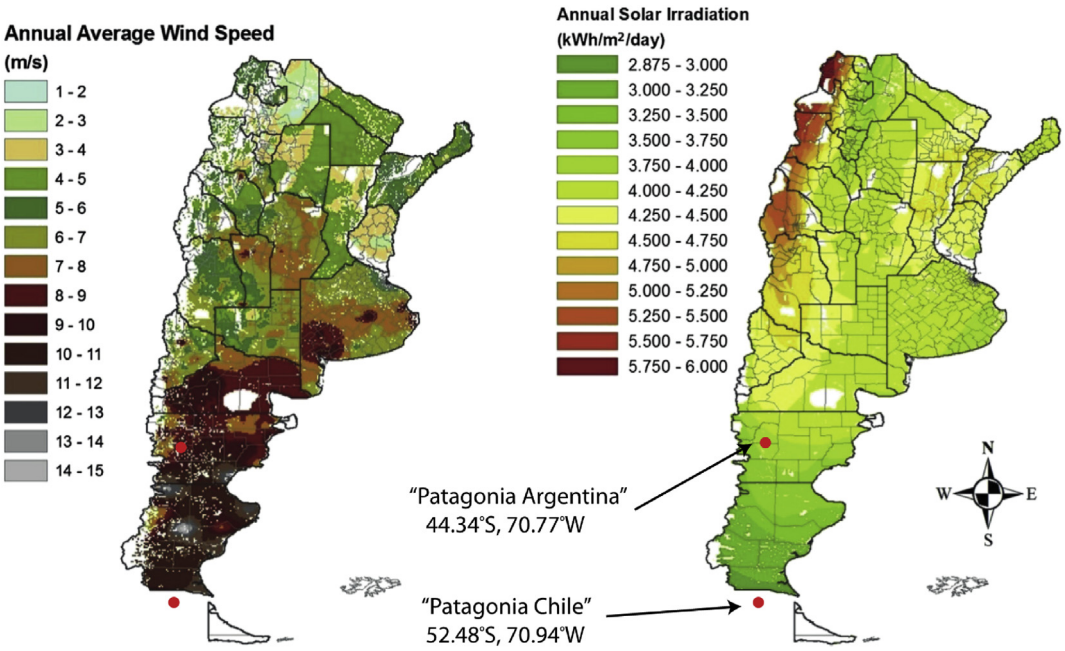

Fig. 2 – Wind and solar resources in Argentina, with land-use restrictions. Wind speed is estimated at 50 m. Source: [24]. Red dots show the "Patagonia Argentina" and "Patagonia Chile" study cases. (For interpretation of the references to colour in this figure legend, the reader is referred to the Web version of this article.)

massive additions of PV capacity, in the 500 MW range. Analysis and forecasts for renewables in both countries are also available in Ref. [32]

Electricity prices in the latest auctions

Following global trends, renewable electricity prices have been going down dramatically in recent years in both countries [33]. Table 2 shows the latest auctions results, in November 2017, for electricity to be supplied by 2023.

The value and market of NH_3

Ammonia is the second most produced synthetic chemical today, after sulphuric acid. In 2017, its production was of 166 Mt [36] of which about 80% were used to produce nitrogen fertilizers. Ammonia represents the second largest demand for pure H_2 after oil refining (about 32 Mt, i.e. 44% in 2018) [6]. As for today's uses, ammonia production (essentially from gas and coal), causes 420 Mt CO_2 emissions, that is, more than 1% of global emissions. Therefore, greening today's ammonia already represents a large opportunity for near-term decarbonisation.

But ammonia is also already the main carrier of hydrogen energy, which avoids the main difficulties and costs of storing and transporting gaseous H_2. Ammonia could thus be a major enabler for renewable energy storage, transport and use [9,37,38]. It may be the most interesting pathway for long-duration storage of chemical hydrogen energy. In particular, ammonia can be combusted with air to provide power, which may represent one solution of choice in many local or regional scenarios towards 100% renewable electricity, to deliver power at times when the wind and solar are not producing enough [39]. Currently, active research is being conducted to find optimal techniques to combust ammonia in gas turbines, or co-combust it with coal or gas in existing steam plants, the two main challenges being to overcome the low flammability, and to ensure the NO_x emissions remain below acceptable standards [40,41]. Also, green ammonia is increasingly being perceived as probably the most cost-efficient option for decarbonizing maritime transport [6,42] and engine manufacturers are preparing for a shift to green ammonia [43].

Since ammonia is a directly useable chemical with an existing market, in agriculture and other end uses, including the explosives industry for mining in Chile, technologies for transporting and storing it are already functional and widely deployed and worldwide, including, e.g., about 5000 km of pipelines in the U.S. Midwest, and a 2500 km long pipeline

Table 1 – The four locations studied. Data source [23].

	Taltal	Calama	Pat. Chile	Pat. Arg.
Latitude (°S)	25.07	22.05	52.48	44.34
Longitude (°W)	69.84	69.08	70.94	70.77
Altitude (m)	2200	2021	331	967
Air density (kg/m^3)	0.95	0.97	1.21	1.13

Table 2 – Latest electricity prices (USD/MWh) in November 2017 auctions. Sources [34,35].

	Chile	Argentina
Avg. price solar	32.5	43.5
Avg. price wind	42.7	41.2
Min. price solar	21.48	40.4
Min. price wind	n.a.	37.3

Please cite this article as: Armijo J, Philibert C, Flexible production of green hydrogen and ammonia from variable solar and wind energy: Case study of Chile and Argentina, International Journal of Hydrogen Energy, https://doi.org/10.1016/j.ijhydene.2019.11.028

from Crime to Ukraine. In general, the costs for transporting or storing ammonia are well lower than those for H_2, and the efficiencies higher [20].

Issues concerning security are also well-known for decades, and the safety track record is excellent. Despite a toxicity that can be lethal to humans at high concentrations, deadly accidents have been very rare for decades of massive use (<3 dead/1 billion pers.). Therefore it is fair to say that "NH_3 is a chemical that should be respected, but not feared" [44].

National strategies for the energy transition and expansion plans for H_2 and H-rich molecules

In Chile, the Long-Term Energy Planning [45] foresees a doubling of the energy consumption between 2016 and 2050 (p. 71). A carbon tax at 5 USD/t CO_2 is already applied in the electricity generation sector, and, in some prospective scenarios, it is considered to rise to 30 USD/t CO_2 in 2030 (p. 63). Scenarios for the energy matrix in Ref. [45] do not consider a decrease of the installed capacities of fossil fuel based electricity generation, however, progressive phasing-out carbon based generation is underway.

In Chile, hydrogen production is being promoted by the Chilean Economic Development Agency (CORFO). Two international consortia have been created at the initiative of CORFO, both for H_2 use for mobility in mining. The production of green NH_3 is also being pursued in the mining context by the company Enaex, which today imports 360 000 t/yr of NH_3 to produce explosives, and aims at cutting its dependency on price volatility and reduce costs by producing solar-based green ammonia.

In Argentina, only one private initiative for H_2 is today visible: the company Hychico, which has developed wind farm-powered electrolysers, and is currently developing hydrogen cavern storage where methanation occurs due to bacteria [46].

Renewable resources in Taltal and Patagonia Argentina locations

Data sources and technological assumptions

The estimation of power production from renewables depends on the atmospheric physical data, and technological assumptions.

Wind. Concerning wind turbines, as discussed for example in Refs. [47–49], the current trend globally in the industry is to increase the swept areas (i.e. decrease the specific power in W/m^2) for similar wind resources. This has allowed to continuously crank up the capacity factors of newly installed plants, and increase the value of the produced energy [47] because it allows to reduce fluctuations in the production, spreading it over more hours.

For example, the average specific power among U.S. turbines, has declined from 395 W/m^2 for projects installed in 1998–1999 to 230 W/m^2 for projects installed in 2018 [49] and the majority of installed turbines currently are of class 3. This trend has been accompanied by a continuous increase in the average capacity factor for newly installed turbines, from about 25-30% to 42% today, even though the quality of the wind resources used has declined by about 15% in the same period (see Fig. 39 in Ref. [49]).

In our modelling, for all sites we use hourly data from Ref. [23] assuming hub height 93 m, and we consider two types of turbine. For northern Chile, we use Vestas V 90–2, which are class 2 turbines of specific power 314 W/m^2, similar to the Vestas 112–3 (with 3075 kW generator) of specific power 312 W/m^2, which are installed in the 99 MW Taltal Enel Green Power plant [50]. However, as mentioned above, the data in Ref. [23] have been noticed to overestimate the resource in the North. Thus, we expect that, in the near future, the best options to optimally exploit the wind potential in northern Chile, should probably rather be class 3 turbines. For our two modelled southern Patagonia locations, due to the extremely strong wind, we consider Nordex 100–3.3 turbines, which are class 1 and have specific power 420 W/m^2, as summarized in Table 3.

As for technical losses, Ref. [51], considering wake effects due to multiple turbine siting, (maintenance) and aging, assumes a factor of reduction. In Ref. [52], the losses (including wake effects, electric and transmission losses) are estimated to 15%, and the availability of the plant to 98%. In our modelling, we assume technical losses of 15% for the southern locations, and 20% for the North, to account also for the overestimation of wind speeds in Ref. [23].

For all locations, both for wind and solar data, we use data for 2013, which is the latest year available in Ref. [23]. Because inter-annual variability is important for wind, in Table 4 we show the deviation of the capacity factors in 2013, used in this work, compared to the climatic average over 1980–2013. The deviation is significant only in the Patagonia Chile case, but the model displays there a sustained increase of the capacity factor over the period, and the 2013 data are good enough to represent present conditions.

Solar. For solar power production, we use data from Ref. [53], assuming 1-axis azimuthal tracking with and zero tilt. In Ref. [21], a loss factor of 15% was used to take into account all technical losses, although in Ref. [54], larger losses of 20–40% are discussed. For all our locations, we assume an overall technical loss factor of 15%.

Note that both for solar and wind, even though technical losses in real plants may be higher in average than our assumption of 15%, their levelized impact over the plant lifetime is lower, because their performance is systematically better in their first half-life of operation [49,54], and the

Table 3 – Wind turbines assumptions for Northern Chile (class 2) and southern Patagonia (class 1).

	Vestas 90–2 (class 2)	Nordex N 100–3.3 (class 1)
Rotor diameter (m)	90	100
Turbine power (MW)	2	3.3
Hub height (m)	93	93
Specific power (W/m^2)	314	420
CAPEX (USD/kW)	1300	1200

Please cite this article as: Armijo J, Philibert C, Flexible production of green hydrogen and ammonia from variable solar and wind energy: Case study of Chile and Argentina, International Journal of Hydrogen Energy, https://doi.org/10.1016/j.ijhydene.2019.11.028

Table 4 – Deviations of wind capacity factors in 2013 from the 1980–2013 average. Source: [23].

	Taltal	Calama	Pat. Chile	Pat. Arg.
Deviation from 1980 to 2013 (%)	−2.5	+1	+19	−2.5

production and revenues in earlier years of life has higher economic value than in later years.

Analysis of renewable energy resources

Taltal. Fig. 3A and B shows the estimated wind and solar resources for 2013 in our Taltal location. Interestingly, Fig. 3A. a shows that the average day cycle has good complementarity with the solar cycle, as wind blows strongly from 10 p.m. to 8 a.m. In Fig. 3A. b and d, one sees that the wind is also more intense in winter (June–September), opposite to the solar radiation. Note that the occurrence of night winds is also interesting in other areas in northern Chile, such as the area of Calama, where the wind variability is also not only seasonal and synoptic (days to weeks), but has a marked thermal (daily) cycle. In Fig. 3A. c, one sees that the load statistics has accumulations near 0 and the maximum at 80% (due to our assumption of 20% losses), and is continuously distributed in between. The large number of hours (>3000) with 80% load, is partly an artefact, due to the above-mentioned overestimation of wind speeds by the model [21].

Fig. 3B shows the Taltal solar resource, with data from Ref. [53], assuming 15% technical losses, which explains the maximal values at 0.85 on Fig. 3B. c. Solar electricity production in Taltal is very stable year round, as seen in Fig. 3B. b and d: only 8 days in 2013 had capacity factors under 20%. The average day cycle (Fig. 3B. a) has very steep slopes at the beginning and end of the day, typical of 1-axis tracking PV plants, which results, in Fig. 3B. c, in a concentration of load statistics at 0% (night) and near the maximal value of 85%.

Patagonia Argentina. Fig. 3C and D shows the wind and solar resource in our Patagonia Argentina (Chubut) location. The wind is extremely strong, with an average capacity factor of 52.7% (including the 15% losses). The average cycle is rather flat both daily and yearly (Fig. 3C. a, b, d). However,

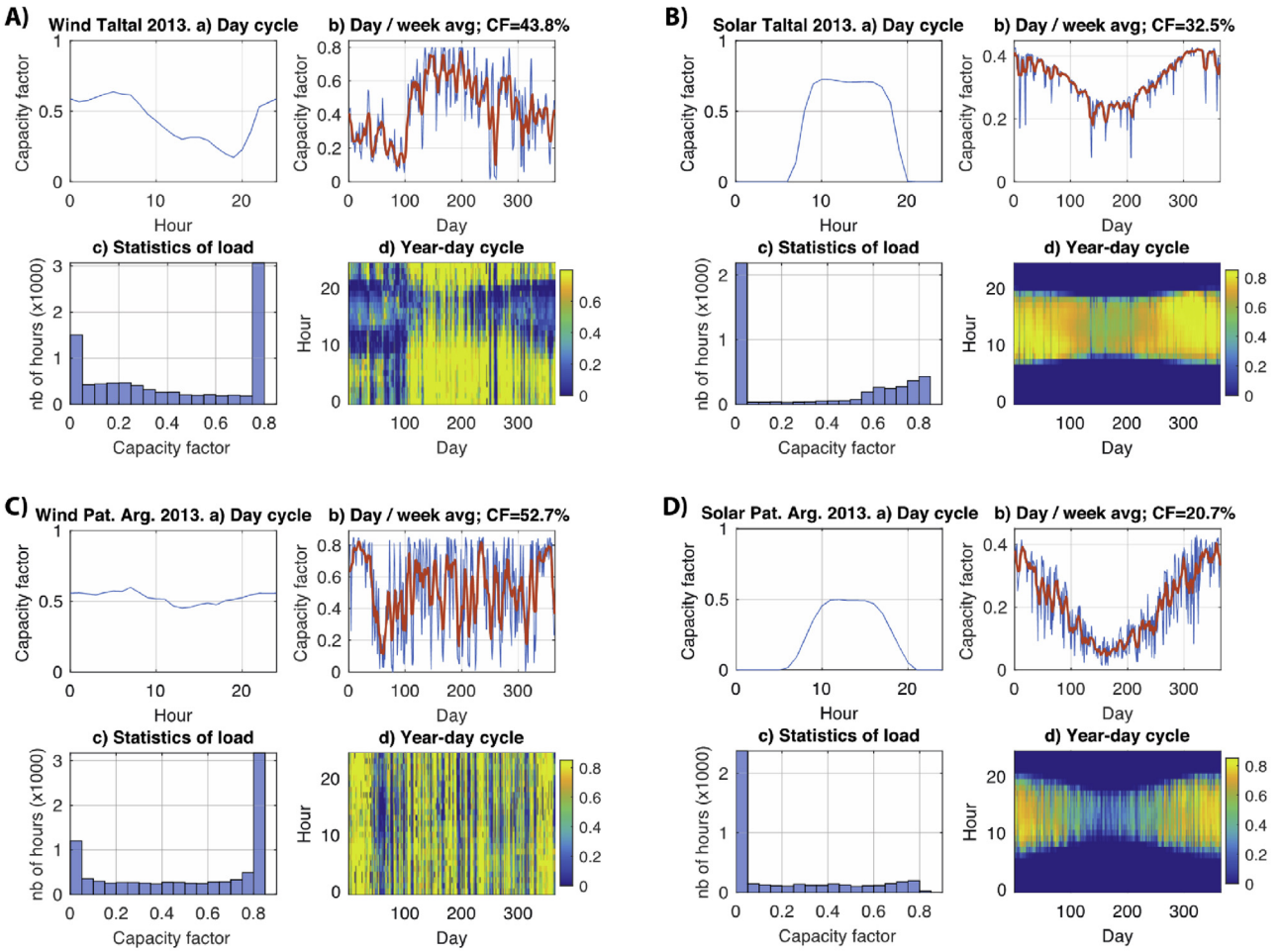

Fig. 3 – Wind and solar resources in (A, B): Taltal, Chile and (C, D): Patagonia Argentina. In each panel: a) Average daily cycle. b) Yearly cycle with day (blue) and weekly average (red). c) Load statistic, bins width: 5%. d) Year-day cycle. Data sources [23,53]. (For interpretation of the references to colour in this figure legend, the reader is referred to the Web version of this article.)

Please cite this article as: Armijo J, Philibert C, Flexible production of green hydrogen and ammonia from variable solar and wind energy: Case study of Chile and Argentina, International Journal of Hydrogen Energy, https://doi.org/10.1016/j.ijhydene.2019.11.028

fluctuations can be very strong on the daily and weekly scale, as seen on Fig. 3C. Note that, in the 6.3 MW Diadema Wind Park in eastern Chubut Province (one of the oldest in Argentina), an average net CF of 47.7% over 2012–2017 was reported [46]. Considering that those turbines are Enercon 44–900 (44 m rotor diameter and 900 kW turbine) at only 45 m height [55], and a very high specific power of 592 W/m^2, brings good credibility to the performance of 52.7% in our model.

The solar resource, shown on Fig. 3D, is weaker, and has a marked yearly cycle with a minimum in winter months (Fig. 3D. b and d).

Optimized production of H_2 from hybrid wind and solar energy

Description of the model

To estimate the production costs of H_2 in Chile and Argentina, we use the economic assumptions in Table 5, including Capital expenditures (*CAPEX*), operational expenditures (*OPEX*), and weighted average capital cost (*WACC*). All our assumptions are conceived for the short term (2020).

Electrolyser. The electrolyser is assumed to be alkaline, with perfectly flexible behaviour, i.e., it can follow in real time the variable electricity supply and maintain a constant efficiency $\eta = 70\%$ relative to the lower heating value (LHV) of hydrogen E_{H2}=33.3 kWh/kg. Such assumptions are consistent with latest technologies reported, e.g. in Ref. [56] where the load range is 10–110%, and for which the maximal ramping rates (up or down) of ± 20%/s is largely sufficient to follow wind or solar variations from utility-scale RE farms. According to Refs. [57,58], 70% efficiency seems optimistic but it is in fact realistic given recent achievements and current progress. Furthermore, efficiencies at partial load are usually higher than at full load (e.g. 67%), which increases the effective average efficiency for renewable power with a statistically important number of hours with partial load [16].

The *CAPEX* assumed is higher than the 450 USD/kW given in Ref. [59] for 2023 to account for installation, but lower than values given in Refs. [57,58]. We can assume that cost reductions by scaling should go fast in the next years, because large scale electrolysers are still in development. In the near future, industrials and the review [60] claim that the large scale (>10 MW) PEM electrolysers can have the same cost reductions as alkaline electrolysers did, so similar prices can be expected for both technologies.

Table 5 – Techno-economic parameters for the electrolysers and solar and wind power plants.

	Value	References
CAPEX electrolyser (USD/kW)	600	[56–62]
OPEX electrolyser (% *CAPEX*/yr)	2	ibid.
lifetime *N* (yr)	30	ibid.
stack lifetime N_s (h)	80 000	ibid.
stack repl. cost (% *CAPEX*)	40	Ibid.
Electrolyser efficiency η (LHV)	70%	ibid.
CAPEX solar (USD/kW)	740	[33,45,63,64]
CAPEX wind (USD/kW)	1200–1300	ibid. [49],
OPEX solar (% *CAPEX*/yr)	1.7	[33]
OPEX wind (% *CAPEX*/yr)	2	[33,49]
tech. losses solar	15%	[21,54,65]
tech. losses wind (North/South)	20%/15%	[21,66]
lifetime vRE plants (yr)	25	–
WACC (Chile/Arg.)	7%/10%	–

VRE plants. For the electricity, the *CAPEX* values that we take are roughly in line with [45,63], however we adjusted them so that the obtained *LCOE* are similar to most recent auction prices (see Table 2). In particular, the *CAPEX* for wind plants in Ref. [45] is 1800 USD/kW, but such high values are probably out of date and could not reproduce the lowest price bids for wind energy, both in Chile and Argentina. Our assumptions for *CAPEX* of wind and solar, are aligned with the ones for China in Ref. [64] for 2020, to which we apply a heuristic 20% cost increment. Note that our estimated *CAPEX* in this fashion, are slightly higher than those of 700 USD/kW for solar, and 1100 USD/kW for wind, assumed for 2020 in Argentina in Ref. [67].

In 2016, in the USA, the average *OPEX* for wind power were of 52 USD/kW for *CAPEX* of 1590 USD/kW [49]. According to Ref. [33], *OPEX* for wind can be as low as 20 USD/kW for full-service initial contracts, and rather on the order of 30 USD/kW for full service renewal contracts. We assume 25 USD/kW/yr. According to [IRENA 17], *OPEX* for solar are between 10 and 18 USD/kW. We assume 13 USD/kW/yr.

Financial cost. A higher *WACC* of 10% is assumed for Argentina, to match the higher prices, probably related to the country risk factor, which is known to be higher than in Chile.

Cost calculations. Our model considers a fixed electrolyser nominal size P_{H2}, powered by dedicated solar and/or wind farms of capacities P_{solar} and P_{wind}. For a range values of the ratios $a_s = P_{solar}/P_{H2}$ and $a_w = P_{wind}/P_{H2}$, we compute the levelized cost of hydrogen *LCOH*. For each couple (a_s, a_w), the full hourly data sets of solar and wind electricity production (presented in Energy situation and strategies for renewables and hydrogen) are combined for the year 2013. The total production of H_2 is computed, as well as the total curtailment of electricity (all power produced that exceeds the nominal capcity of the electrolyser), and the hybrid capacity factor, which is the load factor on the electrolyser. Finally the *LCOH* is computed using the costs of electrolyser, electricity, water (including desalination), and oxygen sales as:

$$LCOH(a_s, a_w) = C_{H2} + C_{elec} + (C_{H2O} - C_{O2}), \quad (1)$$

where for each plant element $k = H_2$, wind or solar (H_2 standing for electrolyser), we use the standard annualised formula

$$c_k = CAPEX_k \times (CRF + OPEX_k) \times E_{H2} / (\eta \times n_{hy} \times CF_k), \quad (2)$$

where, *CRF*=WACC x $(1 + WACC)^N/((1 + WACC)^N - 1)$ is the capital recovery factor, $n_{hy} = 8760$ is the number of hours per year, and CF_k is the capacity factor of the considered plant element *k*.

For the electrolyser, the stack lifetime is assumed to be $N_s = 80\,000$ h, in line with published performances [57]. Stack replacement is done at time $N_{rep} = N_s/(n_{hy} \times CF_h)$, where CF_h is the hybrid load capacity factor that effectively is applied to the electrolyser in each location. We thus add to the electrolyser

Please cite this article as: Armijo J, Philibert C, Flexible production of green hydrogen and ammonia from variable solar and wind energy: Case study of Chile and Argentina, International Journal of Hydrogen Energy, https://doi.org/10.1016/j.ijhydene.2019.11.028

$CAPEX_{H2}$ the net present value of stack replacement ($CAPEX_{H2}$ x 0.4) x (1-WACC)^{Nrep}, using for simplicity the WACC as discount factor.

Concerning water desalination, probably required in northern Chile for H_2 production, with the assumptions of [68] for reverse osmosis, (p. 171) of a CAPEX of 7400 USD/m^3/day, fixed OPEX of 3% of CAPEX, electric consumption of 3 kWh/m^3, lifetime of 30 years, and assuming full load electricity at 60 USD/MWh, the cost of water production is $LCOW = 5.9$ USD/m^3, that is, a cost $c_{H2O} = 0.053$ USD/kg H_2, which is small. For simplicity, the cost of water, as well as the value of the produced oxygen, which in Chile can be $c_{O2} = 0.03$ USD/kg O_2 [69], i.e. 0.24 USD/kg H_2, are both neglected in our calculations for all locations. In Ref. [70], the cost of desalination of water is also seen to be negligible.

Optimization procedure. A minimum search is then applied to the matrix $LCOH(a_s, a_w)$, determining the parameters for the optimal hybrid plant in each location (see Fig. 4).

Example of LCOH optimization in Taltal and Patagonia Argentina

Taltal. Fig. 4 shows the LCOH in Taltal, for various combinations of wind and solar plant sizing relative to the electrolyser. The computed levelized costs of electricity $LCOE_s = 26.7$ USD/MWh and $LCOE_w = 35.8$ USD/MWh are in good agreement with the latest auction prices in Chile (see Table 2). The lowest $LCOH^* = 2.12$ USD/kg, is obtained with the optimal combination $a_s^* = 1.18$ solar and $a_w^* = 0.33$ wind.

In this case study where solar electricity is the cheapest, the modest hybridization of solar with some more expensive wind electricity allows to increase the capacity factor of the electrolyser from 41.3% (the best case with only solar, oversized at $a_s = 1.29$), to 51.8%. A fraction $curt^* = 1.8\%$ of the renewable electricity mix is curtailed, and the LCOH is reduced thanks to this hybridization, by 1.6% only.

Patagonia Argentina. In the Patagonia Argentina case, our model yields electricity prices $LCOE_s = 51.8$ USD/MWh and $LCOE_w = 33.8$ USD/MWh, also in good agreement with latest auction prices (see Table 2), projecting upcoming learning and deployment of the technologies. In this location where wind electricity is notably cheaper than the solar, the lowest $LCOH^* = 2.33$ USD/kg is obtained without hybridization, that is, with $a_s^* = 0$, and with a slight oversizing of the wind farm capacity, with $a_w^* = 1.18$, so that the optimal load factor of the electrolyser is 62.2%, with only 0.2% of the electricity curtailed (see Table 6).

Summary of hydrogen production costs

Fig. 5 shows a comparison of the obtained optimal $LCOH^*$ in our four selected locations, and the optimal parameters found are summarized in Table 6. In sum, we note that hybridization can be slightly profitable for H_2 production, only when the electricity costs are close to each other. But for the cases we run, the gain from hybridization (cost reduction) is limited to 1.6%, in Taltal, compared to the best case with only solar. This is because we have treated cases where one resource is strongly dominant on the other.

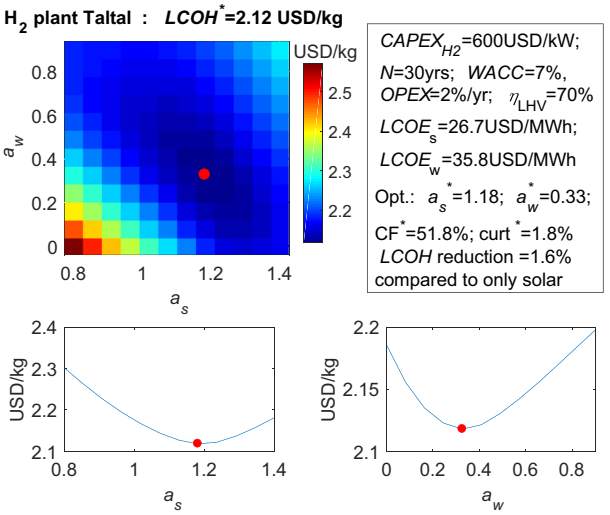

Fig. 4 – Optimization of wind and solar capacities for a hybrid H_2 plant in Taltal. The red dots show the identified optimum. (For interpretation of the references to colour in this figure legend, the reader is referred to the Web version of this article.)

Table 6 – Summary of optimal parameters for hybrid H_2 plants.

	Taltal	Calama	Pat. Chile	Pat. Arg.
Capacity factor solar (%)	32.5	32.4	17.4	20.7
Capacity factor wind (%)	43.8	35.6	51.8	52.7
LCOE solar (USD/MWh)	26.7	26.8	49.9	51.8
LCOE wind (USD/MWh)	35.8	44.1	28	33.8
Capacity solar a_s^*	1.18	1.29	0	0
Capacity wind a_w^*	0.33	0	1.18	1.18
Hybrid load CF* (%)	51.8	41.1	61.2	62.2
curt* (%)	1.8	1.7	0.1	0.2
hybridisation cost reduction (%)	1.6	0	0	0
LCOH* (USD/kg)	2.12	2.16	1.94	2.33

Hybridization of course is more favoured when daily and yearly cycles combine favourably, because they can increase the hybrid capacity factor CF* of the electrolyser. In general, this is not a strong effect, and the temporal correlation between wind and solar productions is small [15]. However, it can be an interesting factor to consider, where the wind has a marked daily cycle, which is often the case in northern Chile, where cycles can be favourable, as in Taltal (see Fig. 3). Running different test cases, we also noted that the interest for hybridization is enhanced when $CAPEX_{H2}$ is larger.

Table 6 allows to visualize the driving ingredients of the LCOH in our four studied locations. First, the lowest LCOH are obtained where electricity is cheapest. In Taltal, with solar at 26.7 USD/MWh, the LCOH is 2.12 USD/kg, however in

Please cite this article as: Armijo J, Philibert C, Flexible production of green hydrogen and ammonia from variable solar and wind energy: Case study of Chile and Argentina, International Journal of Hydrogen Energy, https://doi.org/10.1016/j.ijhydene.2019.11.028

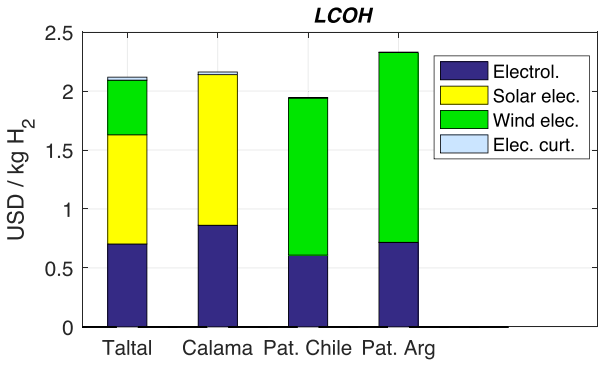

Fig. 5 – Cost structure for the optimal *LCOH* for hybrid H_2 plants in our four locations. Each element includes *CAPEX* and *OPEX* for the considered unit.

Patagonia Chile, with slightly more expensive wind at 28 USD/MWh, the *LCOH* is lower at 1.94 USD/kg. This is due to the effective capacity factor of $CF = 61.2\%$ in Patagonia Chile, larger than the $CF = 51.8\%$ in Taltal. Another remark is that the larger assumed *WACC* in Argentina, prevents from reaching the same low *LCOH* as in Chile, although the quality of the wind in the far South is as good as in Chile.

Optimal flexible production of NH_3 from hybrid wind and solar energy

Description of the model

Modelling a green NH_3 plant, as shown in Fig. 6, is substantially more complex than modelling a green H_2 plant. After H_2 is produced, it has to go through the Haber-Bosch (HB) process, where it is combined with N_2, previously obtained from an air separation unit (ASU), to give NH_3. This combination, usually run on less variable hydropower sources, has actually been the workhorse of the fertiliser industry from 1926 to the 1980s [19].

Table 7 – Techno-economic parameters for flexible Haber-Bosch plant.

	Values	References
$CAPEX_{HB}$ (USD/kW) (LHV H_2 in)	580	[39]
$CAPEX_{ASU}$ (USD/kW) (LHV H_2 in)	224	ibid.
$OPEX_{HB+ASU}$ (% CAPEX/y)	2	ibid.
lifetime (y)	30	ibid.
Elec. HB-ASU (MWh/t NH_3)	0.64	ibid.
Elec. pre-compression (MWh/t NH_3)	0.26	ibid.
flexibility HB total down (% max load)	40/80	[71,72]
flexibility HB up (% max. load)	5	[71]
max ramp (+/- % load/h)	20	[interviews]
cold stop load (%)	0	–
cold stop min. duration (h)	48	–
$CAPEX_{stor}$ cylinders (USD/kWh) (LHV)	12	[39]
$CAPEX_{stor}$ cavern (USD/kWh) (LHV)	0.6	[73]
$OPEX_{stor}$ storage (% CAPEX/y)	1	[39]
Cost elec. firm-up (USD/MWh)	100	–

The Haber-Bosch synthesis loop, in general, is much less flexible than an electrolyser: φ_{HB}, the intake flux of H_2 in the reactor, cannot be varied as rapidly as does φ_{H2}, the flux of H_2 production by the electrolyser. One thus has to include an intermediate storage of H_2, large enough to buffer the fluctuations of H_2 production. For this purpose, we consider pressurised gaseous H_2 storage in steel tanks, which is quite costly, but well mature and available off the shelf. If available, one could also consider underground storage of H_2 in caverns, which is much cheaper. Table 7 summarizes our techno-economic assumptions.

HB synthesis unit. In our model, the power needed for the HB and ASU – at nominal HB load, 0.64 MWh/t NH_3, which is 12.4% of the LHV chemical energy output of 5.17 kWh/t NH_3, and 7.3% of the power π_{H2} flowing in the electrolyser – is taken as much as possible from the renewable power mix as π_{HB}. The required complement of firm-up electricity $\pi_{firm\text{-}up}$ is assumed to cost 100 USD/MWh, whether purchased from the grid or produced locally with one or another form of generation or storage. Note that the power needed for the pre-

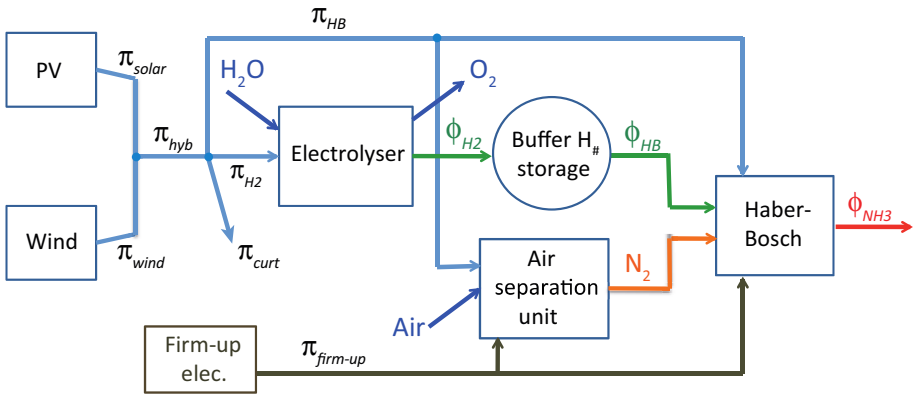

Fig. 6 – Schematic of a green all-electric Haber-Bosch plant. Light blue lines denoted by π show power flows, other lines represent chemical energy fluxes when denoted by φ, or mass flows. (For interpretation of the references to colour in this figure legend, the reader is referred to the Web version of this article.)

Please cite this article as: Armijo J, Philibert C, Flexible production of green hydrogen and ammonia from variable solar and wind energy: Case study of Chile and Argentina, International Journal of Hydrogen Energy, https://doi.org/10.1016/j.ijhydene.2019.11.028

compression of the H_2 before storage (assumed at 60 bars), is here included in the total power π_{H2} needed for the electrolysis, that is, a specific consumption of 1.5 kWh/kg H_2 (0.26 MWh/t NH_3) is added to the $(E_{H2}/\eta) = 47.6$ kWh/kg H_2 that are required in the electrolysis modelled above for H_2 production only, so that the electrolyser efficiency including precompression is $\eta_2 = 68\%$. Our assumptions for the HB CAPEX and OPEX are taken from Ref. [39].

Buffer H_2 storage. For the buffer H_2 storage, reported values cover a wide range from about 200 to 1500 USD/kg depending on the scale and the pressure, with current costs around 500 USD/kg, and ambitious long term targets down to 80 USD/kg [39]. Having in mind rather low pressure storage (at 60 bar) at industrial scale, we take a moderately optimistic assumption of 400 USD/kg (12 USD/kWh). It can be noted that the storage of H_2 is much cheaper than the storage of electricity in batteries, at about 200 USD/kWh, but still much more expensive than the storage of ammonia, at about 0.14 USD/kWh [39]. Note also that H_2 storage could be realised by variable pressure in pipelines, in case transport is needed between the electrolyser and the NH_3 synthesis plant - as will likely be the case for the Engie-Enaex project in Calama, Chile, the electrolysers being planned to lie near Calama in altitude, while the NH_3 synthesis would take place in Mejillones, near the coast [74]. In favorable locations, H_2 storage could also be done in underground salt caverns, which could make the CAPEX for storage as low as 0.6 USD/kWh [73], and could greatly reduce the costs of managing the variability of VRE power sources.

Flexibility: load modulation, enhanced flexibility, cold stops. Standard HB machines today operate at high pressure and high temperature. The syngas (mixture of N_2, H_2 and inerts such as argon) must be compressed to 100–250 bars and heated to about 400–500 °C before entering the synthesis loop [20,75]. The required compressor represents the major part of the $CAPEX_{HB}$. It should be noted, however, that several companies are developing catalysts able to work at lower pressure, so as to make renewables-based HB more agile and possibly less costly, as reported, e.g., in Refs. [76,77] at 10 bar, or in Ref. [78] at 50 bar. In Ref. [76], ramping the load up by about 25% in about 1 min was demonstrated. R&D is also being pursued on electrochemical techniques to produce NH_3 directly from air and water [79], however, all such ideas are in exploratory phase, and their costs are not well defined. Thus, in our modelling we consider only the well demonstrated and established HB scheme. This route is already partially being pursued in the recently announced project by Engie and Yara at Pilbara, Western Australia, where green H_2 from solar power will replace a fraction (about 1%) of the grey H_2 from SMR in the existing HB plant [80], and in the project of H2U and ThyssenKrupp at Port Lincoln, South Australia [81].

We assume that all of the H_2 is transformed into NH_3, although this is not fully exact when working away from nominal conditions [Cheema 18]. Thus the output chemical energy flux is $\varphi_{NH3} = (3/17)\ \mathrm{x}\ (E_{NH3}/E_{H2})\ \varphi_{HB} = 0.88\ \varphi_{HB}$, due to the fact that the HB reaction is exothermic.

We define a "standard flexibility" case, where the maximal reduction of φ_{HB} from its maximum is 40%, and the HB-ASU is modelled to work at 3 discrete levels: 100%, 80% and 60% of the maximal flux φ_{HB}^{max}. This assumption for flexibility is realistic with present technologies, according to plant manufacturers (see, e.g. Ref. [82], (p 694) [72]). It is important to note that including no flexibility at all would lead to anomalously high costs (see below Figs. 7 and 8). In agreement with our interviews with manufacturers, we set the maximal rate of change at 20%/hour (relative to the nominal flux). Since, as illustrated below, the largest needs for buffer H_2 storage are related to renewable power variations at the seasonal or synoptic timescales (see Figs. 7 and 8), for example, a week without wind (see Fig. 8b), we find that the maximal ramping rates are not a key limiting factor.

In addition to our "standard flexibility" case, we consider the possibility of an "advanced flexibility" mode, with 80% possible reduction for φ_{HB} from its maximum. According to several interviewed manufacturers and a recent patent [72], a 80% flux reduction is feasible, with ramping times on the order of a few hours. Also, the recent work [71] carried a rigorous analysis of the parameter envelopes for the HB loop with standard parameters, focusing on the conditions to maintain the autothermal behaviour. Six adjustable parameters were studied one by one, and the flexibility that they allowed was quantified. The H_2 : N_2 ratio was found to give the largest flexibility in terms of H_2 intake flux, allowing to reduce it by 67%, when varying it from the standard 3 : 1, to 1.18 : 2.82. Allowing to vary several parameters at the same time, the authors expect down flexibility of up to 80% to be reasonably achievable. It can be noted, as well, that upwards flexibility up to about +10% without losing too much of efficiency, was also possible, varying the intake of inerts (argon) in the gas blend, or increasing the pressure. In our modelling, we also allow for 5% upwards flexibility.

It should be stressed that the efficiency of the HB loop is expected to be reduced when its load is varied away from nominal conditions. To take this into account, we assume that the electricity consumption of the HB-ASU has a fixed component of 20% of the nominal (using 0.64 MWh/t NH_3), and a variable component proportional to the intake flux φ_{HB} of hydrogen in the reactor. This modelling is rough, however, as is clear below (see Fig. 9), the electrical consumption of the HB machines is a rather secondary component of the total LCOA. Hence, our approximation is justified in the present exercise.

In our "advanced flexibility" mode, we also include the possibility to realize "cold stops", that is, to shut down the autothermal HB reaction completely to 0%. According to manufacturers, this process, contrary to load modulation, cannot be realised rapidly: shutting down and starting again involves a waiting time of several days. In our model, we implement this possibility in relation with the weather forecast. We assume that good knowledge of the weather, and that renewable power production estimates are available for several days ahead. If the predicted integrated future production during the next 48 h is lower than a threshold, the plant is shut down, and remains shut down for at least 48 h.

Cost computation. The levelized cost of ammonia *LCOA* depends, as the *LCOH*, on the sizes a_s and a_w of the solar and wind power plants relative to the electrolyser capacity P_{H2}, but also, on the capacity of the HB machine P_{HB}, and its relative size $a_{HB} = P_{HB}/P_{H2}$. We define the more meaningful factor

Please cite this article as: Armijo J, Philibert C, Flexible production of green hydrogen and ammonia from variable solar and wind energy: Case study of Chile and Argentina, International Journal of Hydrogen Energy, https://doi.org/10.1016/j.ijhydene.2019.11.028

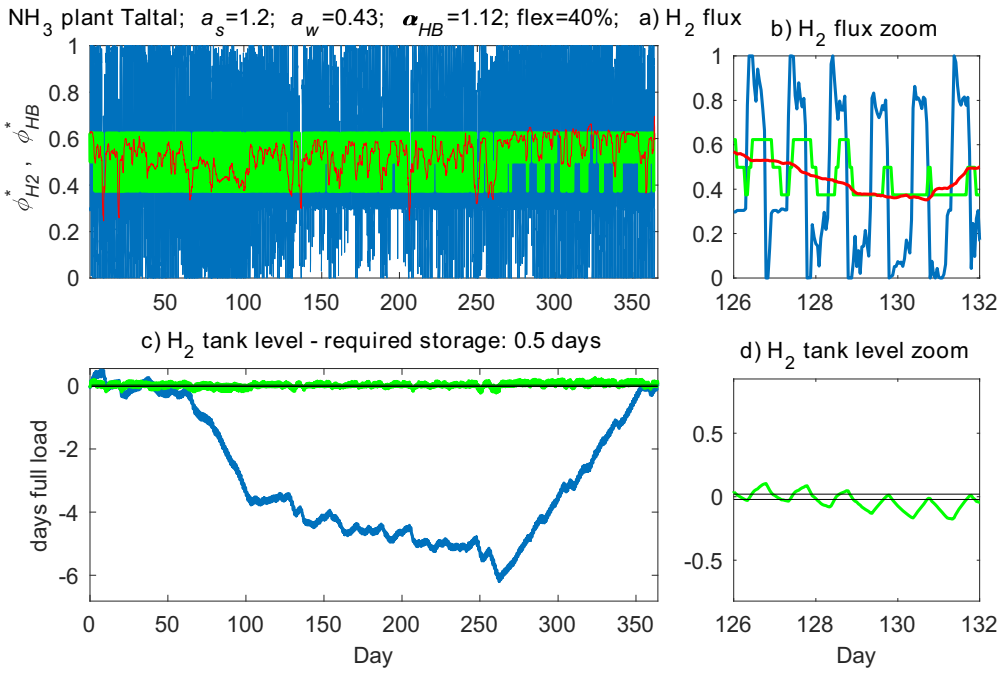

Fig. 7 – Optimal plant for flexible NH_3 production in Taltal, with 40% flexibility. a) Hourly H_2 production flux from the electrolyser φ_{H2}^* (blue), daily average of φ_{H2}^* (red), and hourly HB flux φ_{HB}^* (green), all normalized to the maximal electrolyser output $\eta_2 P_{H2}$. b) Zoom. c) H_2 storage level, without flexibility (blue), and with 40% flexibility (green). Black horizontal lines show the trigger level (±0.5 h full load) to change the HB load level. d) Zoom. (For interpretation of the references to colour in this figure legend, the reader is referred to the Web version of this article.)

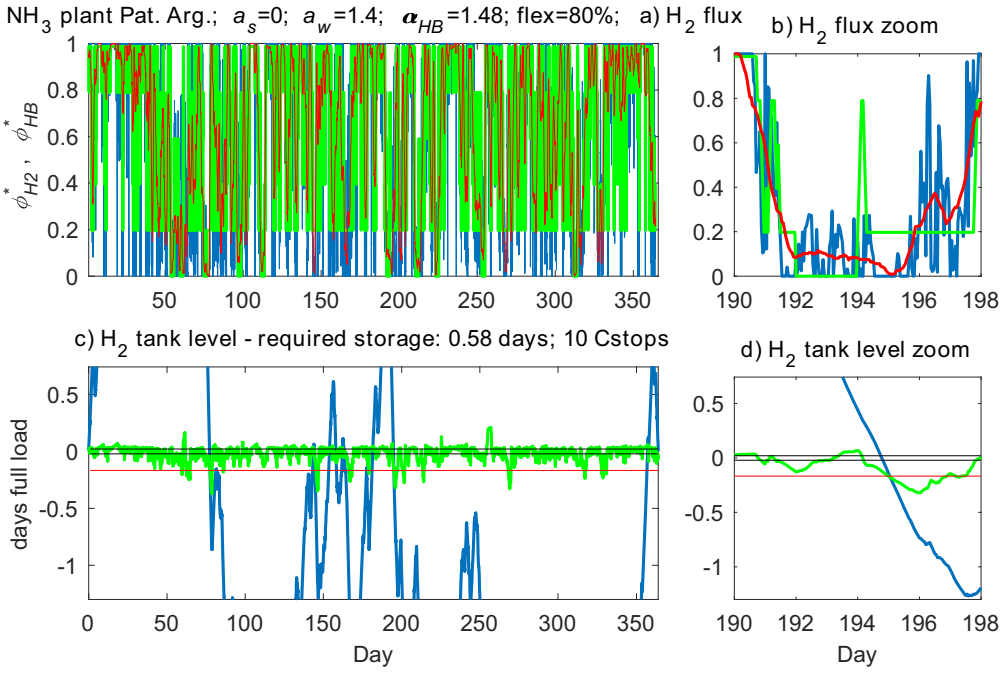

Fig. 8 – Optimal flexible NH_3 production in Patagonia Argentina, with 80% flexibility + stops. a-d) Same as in Fig. 7. In c and d, the red horizontal line shows the tank level below which a stop can be triggered. (For interpretation of the references to colour in this figure legend, the reader is referred to the Web version of this article.)

Please cite this article as: Armijo J, Philibert C, Flexible production of green hydrogen and ammonia from variable solar and wind energy: Case study of Chile and Argentina, International Journal of Hydrogen Energy, https://doi.org/10.1016/j.ijhydene.2019.11.028

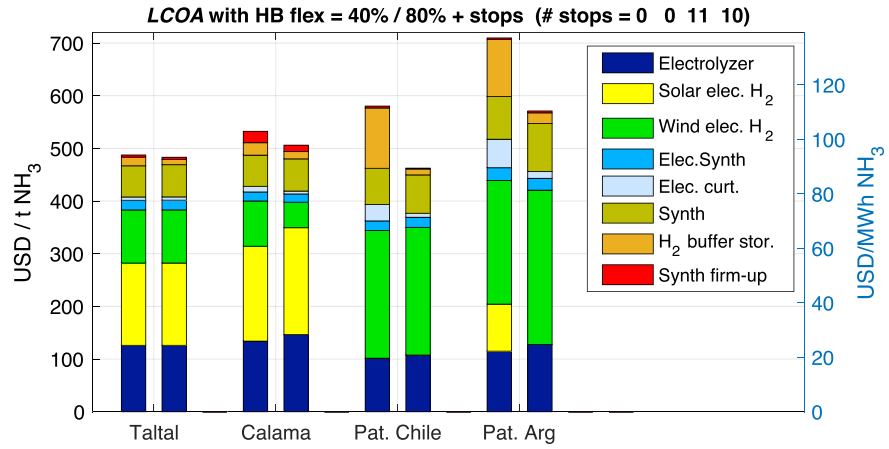

Fig. 9 – Comparison of optimal *LCOA* for hybrid NH_3 plants. For each location the left bar is standard flexibility (40%) and the right bar advanced flexibility (80% + stops). Each element includes *CAPEX* and *OPEX* for the considered unit.

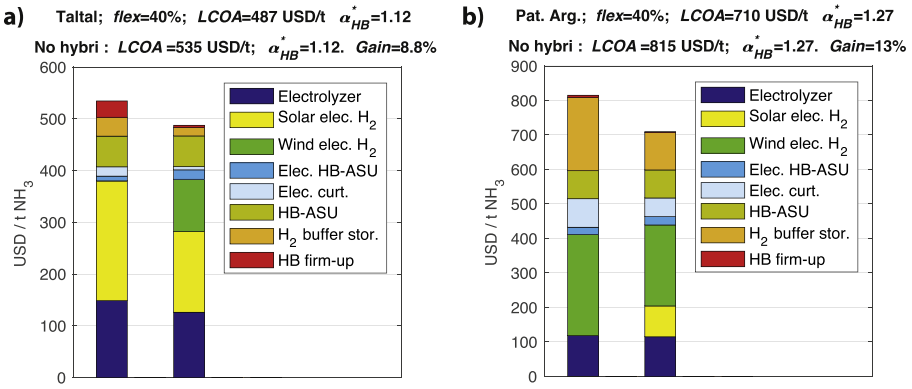

Fig. 10 – Analysis of hybridization gain for NH_3 production in a) Taltal and b) Patagonia Argentina, with standard flexibility (40%). For each location, left bars show the cost splitting for optimal single technology case, and right bars for optimal hybrid case.

$$\alpha_{HB} = \alpha_{HB} / <\varphi_{H2}> = 1/CF_{syn}, \quad (3)$$

that expresses the oversizing of the HB capacity with respect to the mean flux of H_2 production by the electrolyser and which is, by definition, the inverse of the capacity factor of the HB synthesis reactor CF_{syn}. It can be noted that $\alpha_{HB} = 1$ corresponds to the situation where the H_2 buffer storage is sufficiently that it absorbs all the fluctuations in H_2 production, so that the HB operates all year atconstant flux. Defining $CF_{H2} = <\pi_{H2}>$ the load factor on the electrolyser, in this limiting case one would have $a_{HB} = \eta_2\ CF_{H2}$.

For each combination of the 3 optimization parameters (a_s, a_w, α_{HB}) we compute the LCOA as:

$$LCOA(a_s, a_w, \alpha_{HB}) = C_{H2} + C_{elec} + C_{HB-ASU} + C_{firm-up} + C_{stor} + (C_{H2O} - C_{O2}), \quad (4)$$

where $c_{HB\text{-}ASU}$ is the cost of the HB-ASU unit, $c_{firm\text{-}up}$ the cost of the firm-up electricity for the HB-ASU which cannot be obtained from the renewable power mix, and c_{stor} is the cost of the buffer H_2 storage. We evaluate the latter from the full yearly curve of the tank level (see Fig. 7c), computing the minimal required tank size $tank_0$ = max(*tank*) - min(*tank*), where *tank*(i), is the level of H_2 in the buffer tank for each hour i = 1, …, 8760 of the year, and where at each hour step, the variation of the tank level is *computed as:*

Table 8 – Optimal parameters for hybrid NH_3 plants with standard HB flexibility of 40%.

Flexibility 40%	Taltal	Calama	Pat. Chile	Pat. Arg.
Capacity solar a_s*	1.2	1.3	0	0.86
Capacity wind a_w*	0.43	0.34	1.57	1.36
HB oversizing α_{HB}*	1.13	1.13	1.36	1.27
Hybrid load CF* (%)	52.8	49.2	67.6	72
*curt** (%)	2.2	3.7	11	13
*stor** (days full load)	0.5	0.66	4.4	3.5
*firm-up** (% of HB elec.)	6	15	5.3	3.8
hybridization cost reduction (%)	8.8	5.4	0	13
LCOA* (USD/t)	487	521	580	710

Please cite this article as: Armijo J, Philibert C, Flexible production of green hydrogen and ammonia from variable solar and wind energy: Case study of Chile and Argentina, International Journal of Hydrogen Energy, https://doi.org/10.1016/j.ijhydene.2019.11.028

Table 9 – Optimal parameters for hybrid NH_3 plants with advanced HB flexibility of 80% + stops.

Flexibility 80% + stops	Taltal	Calama	Pat. Chile	Pat. Arg.
Capacity solar a_s*	1.2	1.3	0	0
Capacity wind a_w*	0.43	0.17	1.36	1.36
HB oversizing α_{HB}*	1.18	1.18	1.48	1.48
Hybrid load CF* (%)	52.8	44.5	63.3	63.9
*curt** (%)	2.2	2	2.8	3.9
*stor** (days full load)	0.31	0.35	0.41	0.58
*firm-up** (% of HB elec.)	6	18	2.3	5.1
hybridization cost reduction (%)	5.4	1.4	0	0
LCOA* (USD/t)	483	506	462	571

$$tank(i+1) - tank(i) = \varphi_{H2} - \varphi_{HB} \quad (5)$$

Note that $tank(1) = 0$, i.e., the tank level is set to 0 for the first hour of the year, but the absolute value of the tank variable is arbitrary, i.e., only its maximal and minimal values are relevant and determine the required storage capacity to be installed.

From interviews with manufacturers, we find that buffer storage for N_2 is already part of existing ASU, and is not a significant addition to *CAPEX* if about 1 day of production is required as buffer capacity, therefore, we do not consider any variation in the size of the ASU relative to the NH_3 production capacity.

Optimization procedure. The determination of optimal relative sizes of plant sub-units is analogous to the one for H_2 plants: we firstly compute the *LCOA* for a 3-dimensional matrix (a_s, a_w, α_{HB}), and then find the optimal combination yielding the minimum *LCOA*.

The summary of our hybrid NH_3 plant optimization results is presented below in Fig. 9 and Tables 8 and 9. Before commenting the whole set of results, we analyse two modelled examples of flexible NH_3 synthesis, with standard and advanced flexibility.

Example 1: NH_3 plant in Taltal with standard flexibility (40%)

Fig. 7 shows the behaviour of the found optimal hybrid NH_3 plant in Taltal, Chile, in the standard flexibility case. Fig. 7. a shows the hourly production flux of H_2 normalized to maximal electrolyser output $\varphi_{H2}{}^* = \varphi_{H2}/(\eta_2 P_{H2})$ (blue curve), as well as its daily average (red curve) and the intake flux of H_2 in the HB reactor with the same normalization $\varphi_{HB}{}^* = \varphi_{HB}/(\eta_2 P_{H2})$. In the zoom of Fig. 7. b, one sees how $\varphi_{HB}{}^*$ (green curve) follows, with a delay of a few hours, the variations $\varphi_{H2}{}^*$ *(blue curve)*, going up and down from 100% to 60% during most days.

On Fig. 7. c, we see that, without flexibility (blue curve), the required storage tank size, i.e., the difference between the maximal and minimum tank levels during the year, would be about 6 days of H_2 production at full load, which would be prohibitively costly (see also Fig. 11). And we see that this storage need is dominated by the seasonal cycle. On the contrary with 40% flexibility (green curve), the seasonal cycle is completely absorbed, because in this location the seasonal cycle of the optimal RE mix, mostly based on solar, has an amplitude smaller than 40%, and the maximal and minimal tank levels are due to fluctuations at shorter time scales, typically, one or few days with less sun, and the storage need is only 0.51 days equivalent full electrolyser load. The daily cycle of the solar, well visible on Fig. 7b and d, induces a storage need that is about ± 3 h of full load.

Example 2: NH_3 plant in Patagonia Argentina with advanced flexibility (80% + stops)

Fig. 8 shows the behaviour of the hybrid optimal HB plant in Patagonia Argentina, with 80% flexibility. In Fig. 8. b, one sees how the HB flux $\varphi_{HB}{}^*$ (red curve) follows closely the hourly H_2 production flux $\varphi_{H2}{}^*$ (blue curve). In this simulation, 10 "cold stops" to 0% flux (of minimal duration 48 h) are recorded, one of them being visible in Fig. 8. b. These stops are triggered when the tank level (green curve in Fig. 8c and d) goes below the red line level, on the condition explained above, that the tank will not fill up too fast during the minimum stop duration of 48 h.

In Fig. 8. a and b, one clearly sees how more flexibility implies more HB capacity oversizing. Indeed, the average of the working flux $\varphi_{HB}{}^*$ is substantially smaller than its maximal value (which is 5% higher than its nominal value), so that the optimal HB oversizing factor is now $\alpha_{HB}{}^* = 1.48$ (and the capcity factor of the HB rcactor $CF_{syn} = 68\%$) while it is only $\alpha_{HB}{}^* = 1.23$, (and CF_{syn}=81%) in the standard flexibility case for Patagonia Argentina (see Table 8).

Summary of optimal NH_3 production costs

Fig. 9 summarizes the optimal LCOA in our four modelled locations, for buffer storage of H_2 in steel tanks, in the standard (left bars) and advanced (right bars) flexibility cases. The found optimal parameters are summarized in Tables 8 and 9

Several general observations can be made from Fig. 9. First, concerning hybridization, we note that it is substantially more favoured for NH_3 plants than for H_2 plants (see Fig. 5), especially at lower flexibility, where hybrid renewables mixes occur in all locations but Patagonia Chile, providing cost reductions (gains) ranging from 5% to 13%, which is substantially more than the maximum of 1.6% found for H_2 production in Taltal (see Table 6).

A second remark concerns the very large cost of the H_2 buffer storage for the wind-dominated Patagonia locations, when flexibility is limited to "standard". Indeed, in both southern cases, where the wind variability is very strong, large buffer storage capacities of 4.4 and 3.5 days equivalent full load are needed with standard flexibility (see Table 8). As this is very costly, the optimal configuration requires substantial oversizing of the renewable power supply, leading to hybrid load factors of 67.6% and 72% (see Table 8), and large fractions of 11% and 13% of curtailed electricity. Only with such oversizing can the variability of the wind power and thus, the storage costs be reduced.

A third remark is that advanced flexibility (80% + stops) strongly reduces the costs of H_2 storage, especially in the

Please cite this article as: Armijo J, Philibert C, Flexible production of green hydrogen and ammonia from variable solar and wind energy: Case study of Chile and Argentina, International Journal of Hydrogen Energy, https://doi.org/10.1016/j.ijhydene.2019.11.028

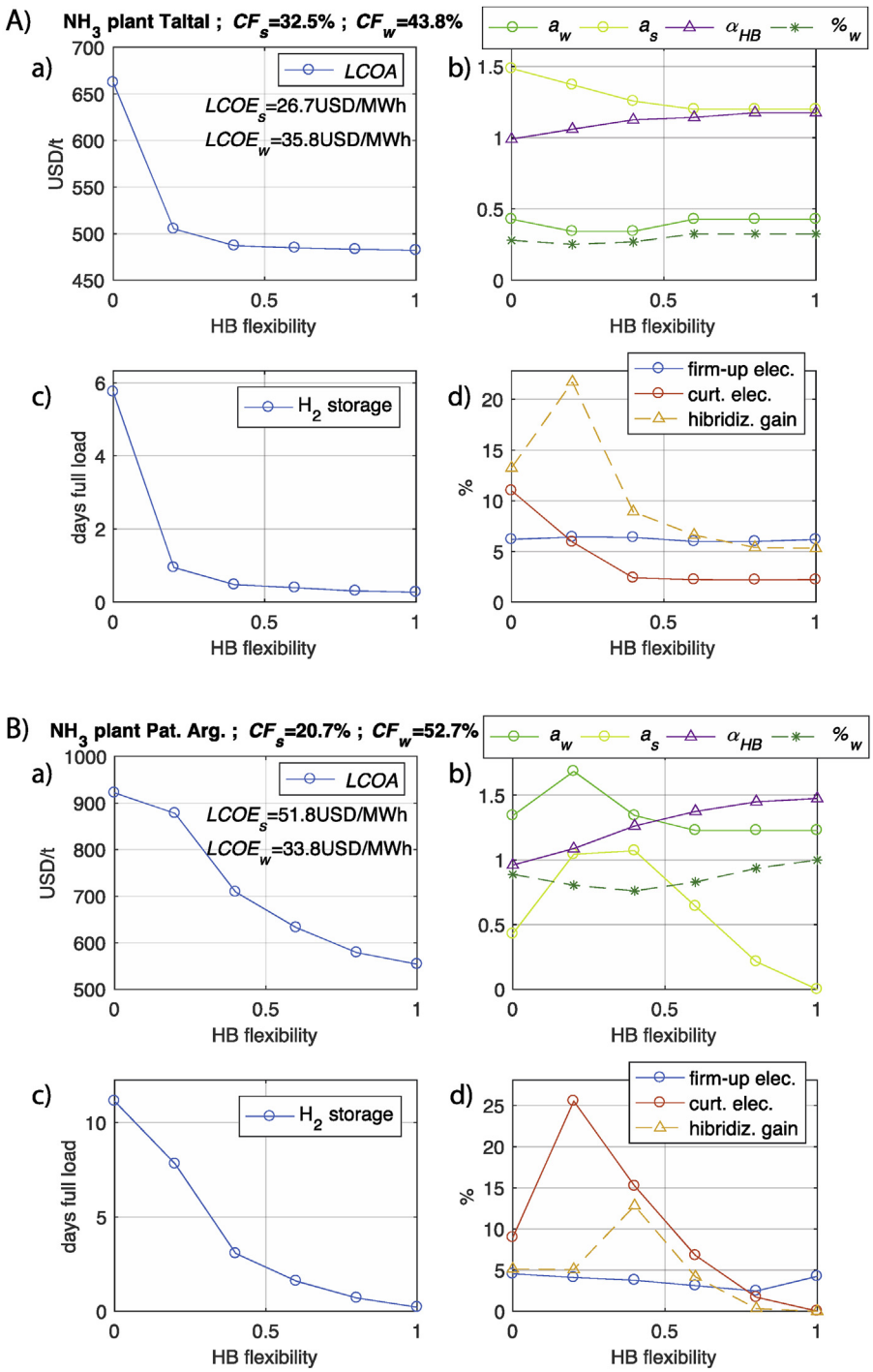

Fig. 11 – Impact of HB flexibility on optimal NH_3 plant in A) Taltal and B) Patagonia Argentina, without cold stops. For each location: a) *LCOA*. b) Capacities a_s and a_w of VRE plants, HB oversizing factor α_{HB} and fraction $\%_w$ of wind in energy mix c) Required H_2 storage capacity. d) Fractions of curtailed and firm-up electricity for HB loop, and LCOA gain by hybridization.

wind-dominated Patagonia locations. There, buffer storage needs are divided almost by 10 by enhanced flexibility, falling from about 4 days (Table 8) to 0.5 days (Table 9) of full load H_2 production. Also, as seen on Fig. 9, because the enhanced flexibility dramatically cuts the costs of the wind fluctuations, it allows including more of this cheaper wind power in the mix. The need to oversize the wind plant capacity in order to mitigate its variability, also vanishes. Indeed, the electrolyser load factors CF_{H2} are reduced on average for Patagonia locations from 70% to 63.5% with enhanced flexibility, and curtailment falls on average from 12% to 3.4%. On the other hand, for both Atacama locations, where fluctuations of the solar resource are much more moderate, advanced flexibility reduces the storage need only slightly, from 0.58 days on average to 0.33 days.

Please cite this article as: Armijo J, Philibert C, Flexible production of green hydrogen and ammonia from variable solar and wind energy: Case study of Chile and Argentina, International Journal of Hydrogen Energy, https://doi.org/10.1016/j.ijhydene.2019.11.028

A fourth remark is that more flexibility results in larger HB oversizing factors a_{HB} (and smaller HB capcity factors CF_{syn}) everywhere, but this effect is particularly strong in the windy Patagonia locations, where a_{HB} increases from 1.3 on average to 1.48, while in the solar-dominated Atacama locations, it only increases on average from 1.13 to 1.18, due again, to the much more regular solar power, compared with the strongly varying wind productions.

Cost performances. With advanced flexibility, Patagonia Chile yields the lowest achievable *LCOA* at 462 USD/t, lower than the 483 USD/t in Taltal, even though the wind at 28 USD/MWh (see Table 6) is more costly than the solar at 26.7 USD/MWh in Taltal. As seen in Fig. 9, the driving factor is the capacity factor on the electrolyser of 63.3% in Patagonia Chile, larger than the 52.8% in Taltal, which reduces the *CAPEX* in electrolyser, even though the *CAPEX* for the HB is larger in Patagonia Chile, where the oversizing of the HB (with respect to the NH_3 production) is 1.48, while it is only 1.18 in Taltal.

Finally, as for the *LCOH*, we see that in Patagonia Argentina, the wind resource is as good or better as in neighbouring Patagonia Chile, but here the solar resource is worth being included in hybridization, when flexibility is low. Still, the unfavourable financial conditions (*WACC* of 10% versus 7% in Chile) make the *LCOA* substantially higher in Argentina.

Analysis of the gain (LCOA reduction) from hybridization

Since hybridization is found to possibly bring about interesting cost reductions, especially at lower HB flexibility, let us now analyse the mechanisms involved, focusing on our two favourite example locations. Fig. 10 shows the *LCOA* cost structure for Taltal (a) and Patagonia Argentina (b), for standard flexibility and for hybrid RE mixes (right bars) versus best single technology cases (left bars). Note that in all cases, optimal configurations are shown, where for single technology cases, the optimization concerns only two (vs three) parameters: the relative size of the RE pant, and of the HB unit.

For Taltal (Fig. 10a), adding wind power increases the load factor end thus reduces the electrolyser cost, despite a slight increase in electricity cost due to uptake of more expensive wind. Teh major part of the 9% reduction of the *LCOA* is obtained by the reduction in the need for firm-up electricity, and for buffer H_2 storage. In fact the key mechanism, is that the added wind electricity, although more expensive, allows to stabilize the power supply, so that less firming electricity has to be acquired, and less H_2 needs being stored.

For Patagonia Argentina (Fig. 10b), the key driver of the 13% cost reduction is the buffer H_2 storage, which is much larger with only wind. In the hybridized case (right bar), even though some more expensive solar is blended with the cheaper wind, the reduced oversizing of the wind plant and thus reduced curtailment makes the spending in electricity equivalent to the case with only wind. Here again, the use of some solar allows to stabilize the wind resource, and reduces the cost induced by its variability.

The impact of HB flexibility

To better understand the impact of HB flexibility on green NH_3 plants, Fig. 11 shows the optimal parameters for hybrid NH_3 plants in Taltal (A) and Patagonia Argentina (B), without cold stops, and flexibility from 0 to 100%. The most important observation is that, in both cases, for increasing HB flexibility, both the *LCOA* and the H_2 buffer storage capacity decrease in a very similar way, which confirms that the H_2 storage is the key cost driver related to the (lack of) flexibility. In the solar dominated Taltal case (Fig. 11A), quite favorably, most of the decrease in H_2 storage size and *LCOA* is obtained within the first 20% of flexibility, which corresponds to the seasonal variability for this RE mix, and which is essentially already available in present day HB units. In the wind dominated Patagonia Argentina case (Fig. 11B), both the *LCOA* and the required H_2 storage decrease rapidly for HB flexibility going from 0 to 40%, which also corresponds to absorbing the seasonal variability, but they also keep decreasing substantially when flexibility goes all the way up to 100%.

In Taltal, the wind energy fraction $\%_w$ (Fig. 11A. b), and thus also the amount of firm-up electricity (close to 6%) are almost unaffected by increasing flexibility. With increasing flexibility, the HB oversizing factor α_{HB} continuously increases from 0.99 to 1.18, while the solar capacity a_s and the curtailed fraction continuously decrease. The gain by hybridization is larger at flexibility less than 40%, i.e., as expected, when the RE variability is costly.

In Patagonia Argentina, for HB flexibility under 40%, the share $\%_w$ of wind in the mix is a bit enhanced, due to the important seasonal variability of the solar (see Fig. 4). However, for flexibility increasing above 40%, one sees a continuous increase in the share $\%_w$ of wind, which is locally the cheapest energy. The HB oversizing also continuously increases from 0.96 to 1.48, as expected for more flexible operation, while the fraction of curtailed electricity continuously decreases from about 20% at low flexibility to almost 0% at 100% flexibility. The fraction of grid firm-up electricity decreases for increasing flexibility, but presents a slight increase for the last point at 100% flexibility, when solar electricity disappears from the mix, due to a sudden increase of the number of day hours with no renewable power supply.

The maximal gain by flexibility (from 0 to 100%), is a reduction of the *LCOA* by 27% in Taltal, and 40% in Patagonia Argentina, the difference being due to the stronger variability

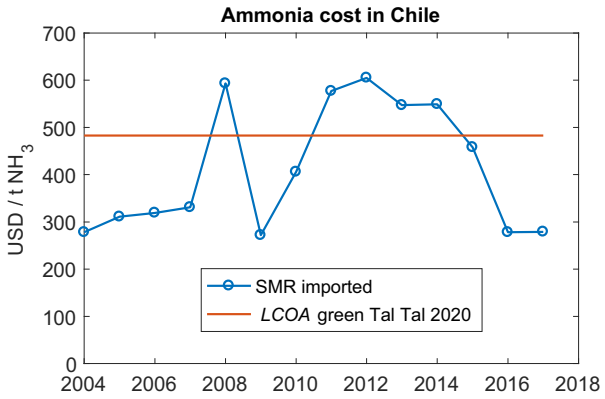

Fig. 12 – Market costs of ammonia in Chile, compared with our Taltal estimate with advanced flexibility at 483 USD/t. Source [83].

Please cite this article as: Armijo J, Philibert C, Flexible production of green hydrogen and ammonia from variable solar and wind energy: Case study of Chile and Argentina, International Journal of Hydrogen Energy, https://doi.org/10.1016/j.ijhydene.2019.11.028

Table 10 – Summary of optimal capacities and *CAPEX*, example case in Taltal, for an ammonia plant producing 35 000 t/yr, with advanced flexibility. (*: MWh).

	HB + ASU	Electrolyser	Solar	Wind	H_2 buffer	Total
Capacity (MW)	27.6	60.2	72.3	25.8	309*	–
CAPEX (MUSD)	21.3	36.1	53.5	33.6	3.7	148

of the wind. Said differently, without any flexibility, the variability of the RE power increases the LCOA by 67% in Patagonia Argentina, and 37% in Taltal, compared to the case with 100% flexibility. These estimates are quite lager than the about 8% cost difference found in [17] for flexibility varying from 80% to 0%, for mostly wind-based ammonia production in the UK.

Strategic view for NH_3 production

Based on these results, NH_3 production in northern Chile seems a particularly low hanging fruit, due to the existence in the area of a mature solar market, with an excellent resource, interesting wind options, available water desalination technology, and large local consumption of ammonia due to mining, in particular for the direct use in explosives (and oxygen as a by-product). Fig. 12 shows the market case, comparing recent prices of imported grey ammonia (from natural gas), and our estimate for 2020 conditions in Taltal with advanced flexibility.

In Patagonia, both Chilean and Argentinian, very promising opportunities could also emerge for producing green H_2 or NH_3 from wind, and perhaps some solar in the northernmost locations (Chubut, Río Negro, Neuquén), possibly firmed-up by some stranded hydro resources that could also help to buffer the variability. Due to the quality of the resource and the vast desert spaces, such cases could aim at large scale export of synthetic fuels via pipelines and ships, for example towards Japan [18].

Finally, for illustration, Table 10 shows the scaled parameters for a 35 000 t/yr green ammonia plant in Taltal, with advanced flexibility. The largest share of the *CAPEX*, and also of the land footprint, would be the 72.3 MW solar farm, complemented by a 25.8 MW wind farm. The required buffer storage tank size is of 309 MWh/E_{H2} = 9.3 t H_2, that is, about or 1 700 m^3 at 60 bars, and the total *CAPEX* would be 148 MUSD.

Discussion

In this work we have developed a methodology that can be applied to any location in the world, provided that reliable meteorological and realistic economic data are available, to compute costs of flexible production of H_2 and NH_3 from variable wind and solar energy.

Our study brings novel understanding about hybridization for RE-based H_2 and alternative fuels production, beyond some general insights provided, e.g. in Ref. [15], where hybrid wind-solar plants were studied only in fixed ratios of capacities. For H_2, we find that combining solar and wind resources can reduce production costs in moderate amounts, e.g., by 1.6% in our most favourable case of Taltal, up to perhaps about 5% in locations with wind and solar resources of similar qualities and costs. On the other hand, for NH_3 production, we find that gains by hybridization can be substantially larger, in the 5–20% range, because it allows to stabilize the RE power supply, and thus reduce the need for expensive buffer storage of H_2 and firming-up electricity for the HB synthesis.

Our work also clarifies the key role of flexibility in the production of green ammonia. In our model, assuming buffer storage of gaseous H_2 in steel tanks, enhanced flexibility continuously reduces the H_2 storage cost and the total *LCOA*. We observe that the cost increase due to RE variability is substantially larger for the strongly variable wind resource: up to 67% in our Patagonia Argentina case with 0% flexibility compared to 100% flexibility. For solar power, which is more regular, the cost increase reaches up to 37% in our Taltal case. Our work also reveals how flexibility can modify the whole structure of the optimal plants considered, and points towards the key value of flexibility in green ammonia projects, and the importance of devoting sufficient R&D to address this major cost driver. Note, of course, that if underground storage of H_2 is locally available, the costs induced by variability and storage could be drastically reduced. Our work also reveals how flexibility can modify the whole structure of the optimal plants considered.

In these locations all boasting world-class wind or solar, we have found that green H_2 and NH_3 could be soon produced at costs almost competitive with the traditional fossil fuel alternatives. Our estimated *LCOH* of about 2 USD/kg, comparable to the estimated 2.16 USD/kg for wind in Argentina in Ref. [18] or the 1.8–3 USD/kg for solar in Northern Chile for 2023 [68], are starting to challenge the 1–1.5 USD/kg for steam methane reforming (SMR) [5,6], and our *LCOA* below 500 USD/t are already commensurate to the 300–600 USD/t market value of imported NH_3 from SMR in Chile. Thus, the expected cost reductions for electrolysers and solar and wind energy, make the production of green H_2 and NH_3, well identifiable business cases in the short term. Factoring in the economic value of price stability (versus fossil fuels price volatility), as well as climate benefits or possibly increased carbon taxes would make the case even more compelling.

Future further analysis could refine the modelling, e.g., including the variable efficiency of the electrolyser at partial load and beyond nominal load. Also, the flexibility assumptions will need to be tested and their costs assessed, in particular concerning the behaviour of the catalysts, in upcoming real world projects.

Acknowledgements

This work was funded by the IEA, thanks to grants from the French government through ADEME, and the German

Please cite this article as: Armijo J, Philibert C, Flexible production of green hydrogen and ammonia from variable solar and wind energy: Case study of Chile and Argentina, International Journal of Hydrogen Energy, https://doi.org/10.1016/j.ijhydene.2019.11.028

government. The views expressed are those of the authors and do not necessarily reflect those of the IEA or its member countries.

REFERENCES

[1] Ramanathan V, Molina L, Zaelke D, Borgford-Parnell N, Xu Y, Alex K, et al. Well under 2 degrees celsius: fast action policies to protect people and the planet from extreme climate change. 2017.
[2] World Bank. Turn down the heat : why a 4°C warmer world must be avoided. 2012.
[3] IPCC. Global Warming of 1.5°C. An IPCC Special Report on the impacts of global warming of 1.5°C above pre-industrial levels and related global greenhouse gas emission pathways, in the context of strengthening the global response to the threat of climate change, sustainable development, and efforts to eradicate poverty. 2018.
[4] UNEP. Emissions Gap Report, vol. 2018; 2018.
[5] Philibert C. Renewable energy for industry. Paris Int Energy Agency; 2017.
[6] IEA. The future of hydrogen. Paris: OECD; 2019.
[7] IRENA. Hydrogen from renewable power: technology outlook for the energy transition. 2018.
[8] Hydrogen IRENA. A renewable energy perspective. 2019.
[9] Andersson J, Grönkvist S. Large-scale storage of hydrogen. Int J Hydrogen Energy 2019.
[10] IEA. WEO 2018. Paris: OECD; 2018.
[11] Götz M, Lefebvre J, Mörs F, Koch AM, Graf F, Bajohr S, et al. Renewable Power-to-Gas: a technological and economic review. Renew Energy 2016;85:1371–90.
[12] Hank C, Gelpke S, Schnabl A, White RJ, Full J, Wiebe N, et al. Economics & carbon dioxide avoidance cost of methanol production based on renewable hydrogen and recycled carbon dioxide–power-to-methanol. Sustain Energy Fuels 2018;2:1244–61.
[13] Tunå P, Hulteberg C, Ahlgren S. Techno-economic assessment of nonfossil ammonia production. Environ Prog Sustain Energy 2014;33:1290–7.
[14] Morgan E, Manwell J, McGowan J. Wind-powered ammonia fuel production for remote islands: a case study. Renew Energy 2014;72:51–61.
[15] Fasihi M, Bogdanov D, Breyer C. Techno-economic assessment of power-to-liquids (PtL) fuels production and global trading based on hybrid PV-wind power plants. Energy Procedia 2016;99:243–68.
[16] Schulte Beerbühl S, Fröhling M, Schultmann F. Combined scheduling and capacity planning of electricity-based ammonia production to integrate renewable energies. Eur J Oper Res 2015;241:851–62.
[17] Nayak-Luke R, Bañares-Alcántara R, Wilkinson I. "Green" ammonia: impact of renewable energy intermittency on plant sizing and levelized cost of ammonia. Ind Eng Chem Res 2018;57:14607–16.
[18] Heuser P-M, Ryberg DS, Grube T, Robinius M, Stolten D. Techno-economic analysis of a potential energy trading link between Patagonia and Japan based on CO2 free hydrogen. Int J Hydrogen Energy 2019;44:12733–47.
[19] Philibert C. Producing ammonia and fertilizers: new opportunities from renewables. Paris: IEA, OECD; 2017.
[20] Bartels JR. A feasibility study of implementing an ammonia economy. Iowa State University; 2008.
[21] Santana C, Falvey M, Ibarra M, García M. Energias Renovables en Chile. El potential eolico, solar e hidroelectrico de Arica a Chiloe. Santiago Chile: MINENERGIA GIZ; 2014.
[22] Ministerio de Energia de Chile. Explorador solar. http://www.minenergia.cl/exploradorsolar/; 2013.
[23] Ministerio de Energia de Chile. Explorador Eólico. http://walker.dgf.uchile.cl/Explorador/Eolico2/; 2013.
[24] Sigal A, Leiva EPM, Rodríguez CR. Assessment of the potential for hydrogen production from renewable resources in Argentina. Int J Hydrogen Energy 2014;39:8204–14.
[25] World Bank. Global wind atlas. n.d. https://globalwindatlas.info.
[26] World Bank. Global solar atlas. n.d. https://globalsolaratlas.info/.
[27] IEA. Countries. n.d. https://www.iea.org/countries/.
[28] IEA. Energy policies beyond IEA countries: Chile 2018 review. Paris: OECD; 2018.
[29] Ministerio de Energia de Chile. Capacidad instalada – energía Abierta. n.d. http://energiaabierta.cl/visualizaciones/capacidad-instalada/.
[30] BNEF. The clean technology fund and concessional finance. 2019.
[31] Wind Power Monthly. The 7 best performing wind markets in 2018. 2019.
[32] IEA. Renewables 2018. Analysis and forecast to 2023. 2018.
[33] IRENA. Renewable power generation costs in 2017. 2019.
[34] ACERA. Análisis ACERA-Resultados del proceso de Licitación 2017/01. 2017.
[35] Ministerio de Energia de Argentina. Resumen de Ofertas adjudicadas RenovAr 2 FASE 1 2017.
[36] FAO. World fertilizer trends and outlook to 2020. 2017.
[37] Bañares-Alcántara R, Dericks G, Fiaschetti M, Grünewald P, Lopez JM, Tsang E, et al. Analysis of islanded ammonia-based energy storage systems. 2015.
[38] Giddey S, Badwal SPS, Munnings C, Dolan M. Ammonia as a renewable energy transportation media. ACS Sustain Chem Eng 2017;5:10231–9.
[39] Ikäheimo J, Kiviluoma J, Weiss R, Holttinen H. Power-to-ammonia in future North European 100% renewable power and heat system. Int J Hydrogen Energy 2018;43:17295–308.
[40] Valera-Medina A, Xiao H, Owen-Jones M, David WIF, Bowen PJ. Ammonia for power. Prog Energy Combust Sci 2018;69:63–102.
[41] Kobayashi H, Hayakawa A, Somarathne KKA, Okafor EC. Science and technology of ammonia combustion. Proc Combust Inst 2019;37:109–33.
[42] Ash N, Scarbrough T. Sailing on solar: could green ammonia decarbonise international shipping? Environmental Defense Fund; 2019.
[43] Laursen RS. Ship operation using LPG and ammonia as fuel on MAN B&W dual fuel ME-LGIP engines. 2018.
[44] Anderson MK. Ammonia safety, a global perspective. 2017.
[45] de Energia de Chile Ministerio. Proceso de Planificación energética de Largo plazo. 2018.
[46] Perez A. Hychico. Clean hydrogen production and renewable energy storage. 2017.
[47] Hirth L, Müller S. System-friendly wind power: how advanced wind turbine design can increase the economic value of electricity generated through wind power. Energy Econ 2016;56:51–63.
[48] Dalla Riva A, Hethey J, Vtiņa A. Impacts of wind turbine technology on the system value of wind in europe. Tech. rep., International Energy Agency; 2017.
[49] Wiser R, Bolinger M, Barbose G, Darghouth N, Hoen B, Mills A, et al. Wind technologies market report 2018. 2018. p. 103.
[50] The Wind Power. Taltal (Chile) - wind farms - online access n.d. https://www.thewindpower.net/windfarm_en_20644_taltal.php.
[51] Brower M. Wind resource assessment: a practical guide to developing a wind project. John Wiley & Sons; 2012.

Please cite this article as: Armijo J, Philibert C, Flexible production of green hydrogen and ammonia from variable solar and wind energy: Case study of Chile and Argentina, International Journal of Hydrogen Energy, https://doi.org/10.1016/j.ijhydene.2019.11.028

[52] Stehly TJ, Beiter PC, Heimiller DM, Scott GN. 2017 cost of wind energy review. National Renewable Energy Lab.(NREL); 2018.
[53] Renewablesninja n.d. https://www.renewables.ninja/.
[54] Marion B, Adelstein J, Boyle K, Hayden H, Hammond B, Fletcher T, et al. Performance parameters for grid-connected PV systems. In: Conf. Rec. Thirty-first IEEE photovolt. Spec. Conf. vol. 2005. IEEE; 2005. p. 1601–6.
[55] The Wind Power. Diadema (Argentina) - wind farms - online access. n.d. https://www.thewindpower.net/windfarm_en_15923_diadema.php.
[56] ThyssenKrupp. Power to gas > water electrolysis > products > Home. Uhde Chlorine eng. n.d. https://www.thyssenkrupp-uhde-chlorine-engineers.com/en/products/water-electrolysis-hydrogen-production/power-to-gas.
[57] Schmidt O, Gambhir A, Staffell I, Hawkes A, Nelson J, Few S. Future cost and performance of water electrolysis: an expert elicitation study. Int J Hydrogen Energy 2017;42:30470–92.
[58] Buttler A, Spliethoff H. Current status of water electrolysis for energy storage, grid balancing and sector coupling via power-to-gas and power-to-liquids: a review. Renew Sustain Energy Rev 2018;82:2440–54.
[59] Lokke JA. Nel Group 2017.
[60] Proost J. State-of-the art CAPEX data for water electrolysers, and their impact on renewable hydrogen price settings. Int J Hydrogen Energy 2019;44:4406–13.
[61] Saba SM, Müller M, Robinius M, Stolten D. The investment costs of electrolysis—a comparison of cost studies from the past 30 years. Int J Hydrogen Energy 2018;43:1209–23.
[62] Parra D, Valverde L, Pino FJ, Patel MK. A review on the role, cost and value of hydrogen energy systems for deep decarbonisation. Renew Sustain Energy Rev 2019;101:279–94.
[63] Comision Nacional de Energía. Informe costos de generación 2019.pdf. 2019.
[64] CNREC. China Renewable Energy Outlook 2018;2018.
[65] Maghami MR, Hizam H, Gomes C, Radzi MA, Rezadad MI, Hajighorbani S. Power loss due to soiling on solar panel: a review. Renew Sustain Energy Rev 2016;59:1307–16.
[66] Staffell I, Green R. How does wind farm performance decline with age? Renew Energy 2014;66:775–86.
[67] Kind S. Argentina - renewables vs. natural gas (economics). https://www.linkedin.com/feed/update/urn%3Ali%3Aactivity%3A6530634661180297216/; 2019.
[68] Tractebel. Oportunidades para el desarrollo de una industria de hidrógeno solar en las regiones de Antofagasta y Atacama: innovación para un sistema energético 100% renovable. 2018.
[69] GIZ. Tecnologías del Hidrógeno y perspectivas para Chile. 2018.
[70] Agora Energiewende and Frontier Economics. The future cost of electricity-based synthetic fuels. 2018.
[71] Cheema II, Krewer U. Operating envelope of Haber–Bosch process design for power-to-ammonia. RSC Adv 2018;8:34926–36.
[72] Ostuni R, Zardi F. Method for load regulation of an ammonia plant. 2016.
[73] Comparison ITP. Of dispatchable renewable electricity options - technologies for an orderly transition. ITPEnergised 2018. http://www.itpenergised.com/wp-content/uploads/2018/11/Comparison-Of-Dispatchable-Renewable-Electricity-Options-ITP-et-al-for-ARENA-2018.pdf. [Accessed 25 September 2019].
[74] Enaex. Private communication. 2019.
[75] Morgan ER. Techno-economic feasibility study of ammonia plants powered by offshore wind. 2013.
[76] Beach J. Starfire Energy : rapid ramp NH3 reactor update. 2018.
[77] Welch A. Starfire Energy : advanced heterogeneous catalysts for renewable ammonia synthesis. 2018.
[78] JGC corp. Demonstration of CO2-free ammonia synthesis using renewable energy-generated hydrogen. 2018.
[79] NH3 fuel association. In: 2018 NH3 fuel conference, session "ammonia energy technology roadmap. NH3 Fuel Assoc; 2018. https://nh3fuelassociation.org/conference2018/.
[80] Engie. ENGIE and YARA take green hydrogen into the factory. https://www.engie.com/en/news/yara-green-hydrogen-factory/. [Accessed 26 September 2019].
[81] Brown T. ThyssenKrupp's "green hydrogen and renewable ammonia value chain. Ammon Ind 2018. https://ammoniaindustry.com/thyssenkrupps-green-hydrogen-and-renewable-ammonia-value-chain/.
[82] Stolten D, Scherer V. Transition to renewable energy systems. John Wiley & Sons; 2013.
[83] Enaex. 2017 annual report. 2018.

Please cite this article as: Armijo J, Philibert C, Flexible production of green hydrogen and ammonia from variable solar and wind energy: Case study of Chile and Argentina, International Journal of Hydrogen Energy, https://doi.org/10.1016/j.ijhydene.2019.11.028